Supplementary Information for

Measurement report: Formation of tropospheric brown carbon in a lifting air mass

Can Wu[1,2], Xiaodi Liu[1], Ke Zhang[1], Si Zhang[1]*, Cong Cao[3,4], Jianjun Li[3], Rui Li[1,2], Fan Zhang[1,2], Gehui Wang[1,2]*

[1]Key Lab of Geographic Information Science of the Ministry of Education, School of Geographic Sciences, East China Normal University, Shanghai 210062, China
[2]Institute of Eco-Chongming, 20 Cuiniao Rd., Chongming, Shanghai 202150, China
[3]State Key Laboratory of Loess and Quaternary Geology, Institute of Earth Environment, Chinese Academy of Sciences, Xi'an 710061, China
[4]School of Marine and Atmospheric Science, Stony Brook University, Stony Brook, NY 11794, USA

[*]Corresponding authors: Dr. Si Zhang, E-mail: szhang@geo.ecnu.edu.cn
Prof. Gehui Wang, E-mail: ghwang@geo.ecnu.edu.cn

List of supporting materials:

1. Two text, Text S1- S2.
2. Four tables, Table S1-S4.
3. Nine figures, Figure S1-S10.

Text S1 UV−vis light absorption measurement

About 8 punches (12 cm^3) form each filter sample was extracted three time under sonication with 15 ml Milli-Q pure water (18.2 MΩ), and the extract was subsequently filtered through 0.45 μm PTFE pore syringe filter to remove the insoluble component in the suspension. A liquid waveguide capillary UV−vis spectrometer equipped with a 1 m long-effective path detection cell was applied to record the light absorption spectra of all extracts. The light absorption spectrum was finally converted into absorption coefficient (abs_λ, M/m) at a particular wavelength (λ) using the following equation.

$$abs_{\lambda} = (A_{\lambda} - A_{700}) \frac{v_1}{v_a \times l} \times \ln(10) \quad \text{Eq.S1}$$

Where A_λ and A_{700} represent the light absorption of the extracts at wavelength λ and 700 nm, respectively. V_1 corresponds to the volume of the extract, e.g., 15 ml; V_a refers to the volume of the air through corresponding to filter punches; l (m) is the absorbing path length. While, ln(10) is used for converting common logarithm that provided by the spectrophotometer to natural logarithm.

Text S2 Positive matrix factorization (PMF) source apportionment

To quantitatively determine the fractional contribution of specific sources to BrC, a PMF receptor model (EPA PMF 5.0 version) coupled with a bootstrap technique was applied here, which has been widely used for the source apportionment of atmospheric pollutants in previous studies. For more details of this method, you can found on the EPA website(https://www.epa.gov/air-research/epa-positive-matrix-factorization-50-fundamentals-and-user-guide). Briefly, WSOC, WSON, SO_4^{2-}, NH_4^+, Mg^{2+}, Ca^{2+}, $abs_{365\ nm}$ and organic tracers (BbF, Bghip and levo.) were regarded as the input variables in the present work. As indicated in our previous study on Mt. Hua(Wu et al., 2022), insignificant change in the corresponding emission sources was revealed during air mass lifting process. Thus, the daytime samples from both sites were added together as one data matrix. Considering Q values and interpretability, four factors were obtained as the optimal solution after numerous testes with three to seven factors, and the input species matched well with simulated ones with significant correlations (R^2>0.88).

Table S1 RF model performance for testing dataset.

	MF site	MS site
R^2	0.92	0.86
MSE	0.003	0.008
RMSE	0.054	0.091
MAE	0.04	0.07

Note: MSE: mean square error; RMSE: root-mean-square error; MAE: mean absolute error.

Table S2. Information and mass concentration (μg m^{-3}) of nitroaromatic compounds detected in this study.

Compounds	Molecular	Formula	CAS number	Abbreviation	MF site	MS site
4-Nitrophenol	139.11	$C_6H_5NO_3$	100-02-7	4NP	2.6±2.6	0.40±0.25
3-Methoxy-4-nitrophenol	153.14	$C_7H_7NO_3$	2581-34-2	3M4NP	0.07±0.05	0.01±0.01
4-Nitrocatechol	155.11	$C_6H_5NO_4$	59030-13-6	4NC	1.6±2.5	0.25±0.67
4-Methyl-5-nitrocatechol	169.13	$C_7H_7NO_4$	68906-21-8	4M5NC	11.4±11.4	1.8±1.3
3-Nitrosalicylic acid	183.12	$C_7H_5NO_5$	85038-1	3NSA	0.01±0.01	0.004±0.01
5-Nitrosalicylic acid	183.12	$C_7H_5NO_5$	96-97-9	5NSA	0.13±0.13	0.012±0.015

Table S3 NH_3 concentrations in different regions of China

Region	Location	Period	Ammonia (μg m^{-3})	Reference
NCP	Beijing	Summer of 2009	29.4±11.9	Meng et al.(Meng et al., 2017)
	Gucheng	Mar.2016-May.2017	22.2±12.8	Kuang et al. (Kuang et al., 2020)
		May-Sep 2013	27.5±42.8	Meng et al. (Meng et al., 2018)
	Luancheng	Dec.2015-Feb.2016	17.2	Pan et al. (Pan et al., 2018)
	Cangzhou	Dec.2015-Feb.2016	22.2	
FWP	Xi'an	Winter of 2016	29±7.3	Wu et al. (Wu et al., 2020a)
		Summer of 2016	38±9.4	
		2006-2007	12.9	Cao et al. (Cao et al., 2009)
	Weinan	Dec.2015-Feb.2016	12.4	Pan et al. (Pan et al., 2018)
	Mt. Hua-MS	Summer of 2020	3.1±1.9	Wu et al. (Wu et al., 2022)
	Mt. Hua-MF	Summer of 2020	27.3±51	
YRD	Shanghai	Autumn of 2019	9.5	Wu et al. (Wu et al., 2023)
		July-Dec 2013, Mar-June 2014	9.4±6.9	Wang et al. (Wang et al., 2015)
		Dec.2019-Jan.2020	9.3±4.0	Lv et al. (Lv et al., 2022)
	Nanjing	Dec.2015-Feb.2016	10.8	Pan et al. (Pan et al., 2018)
	Taihu	Dec.2015-Feb.2016	6.3	
	Lin'an	Sep 2009-Dec 2010	12.5±8.5	Meng et al. (Meng et al., 2014)
PRD	Guangzhou	Dec.2015-Feb.2016	5.8	Pan et al. (Pan et al., 2018)
		Oct-Nov 2004	7.3±6.2	Hu et al. (Hu et al., 2008)
	Dinghushan	Dec.2015-Feb.2016	2.8	Pan et al. (Pan et al., 2018)
	Maoming	Dec.2015-Feb.2016	9.8	
	Hongkong	Autumn 2000	2.3±2.7	Yao et al. (Yao et al., 2006)
TP	Lhasa	Dec.2015-Feb.2016	4.8	Pan et al. (Pan et al., 2018)
	Ali	Dec.2015-Feb.2016	1.7	Pan et al. (Pan et al., 2018)

Note: In some cities, the NH_3 unit is ppb, which was converted by the formula of standard atmospheric pressure and normal temperature in this study. The abbreviations of NCP, FWP, YRD, PRD and TP indicate North China Plain, Fen-wei Plain, Yangtze River Delta, Pearl River Delta and Tibet Plateau, respectively.

Table S4 MAE_{365} of water-soluble BrC in $PM_{2.5}$ among different cities in the world.

Region	Location	Year	Season	MAE_{365}	Reference
NCP, China	Beijing	2011	Winter	1.2±0.1	Cheng et al. (Cheng et al.,
		2010-2011	Winter	1.26	Du et al.(Du et al., 2014)
		2010-2011	Summer	0.51	
	Xingtai	2018-2019	Spring	1.4±0.18	Li et al. (Li et al., 2023a)
			Summer	0.95±0.18	
			Autumn	1.5±0.13	
			Winter	1.9±0.16	
	Jinan (TSP)	2016	Spring	1.00±0.23	Wen et al. (Wen et al., 2021)
	Zhangbei	2016	Spring	1.32±0.34	
	Tianjin	2016–2017	Winter	1.54±0.33	Deng et al.(Deng et al., 2022)
			Summer	0.84±0.22	
FWP, China	Xi'an	2016–2017	Winter	1.2±0.06	Wu et al. (Wu et al., 2020b)
			Summer	1.1±0.2	
		2020	Winter	0.78 ± 0.96	Li et al. (Li et al., 2023b)
	Licun	2017	Winter	0.94±0.28	Li et al. (Li et al., 2020)
			Summer	1.01±0.18	
	Mt. Hua-MS	2016	Summer	0.69±0.2	This study
	Mt. Hua-MF			0.67±0.21	
YRD, China	Changzhou	2018	Winter	0.74	Tao et al.(Tao et al., 2021)
	Yangzhou	2015-2016	Annual	0.75 ± 0.29	Chen et al.(Chen et al.,
	Nanjing	2015-2016	Spring	0.69	Chen et al.(Chen et al., 2018)
			Summer	0.51	
			Autumn	0.55	
			Winter	1.04	
	Shanghai	2018-2019	Winter	1.18±0.42	Zhao et al. (Zhao et al.,
PRD, China	Guangzhou	2012	Winter	0.81	Liu et al.(Liu et al., 2018)
		2018	Winter	1.0 ± 0.21	Zou et al.(Zou et al., 2023)
		2019	Winter	0.34	Wang et al.(Wang et al.,
		2016	Autumn	0.60±0.06	He et al. (He et al., 2023)
	Taipei	2021	Annual	0.86±0.60	Ting et al.(Ting et al., 2022)
TP, China	Lulang	2015-2016	Winter	0.75 ± 0.13	Zhu et al. (Zhu et al., 2018)
	Lhasa	2013-2014	Annual	0.74	Li et al. (Li et al., 2016)
	Southeast TP	2013-2014	Summer	0.27 ± 0.10	Wu et al. (Wu et al., 2020c)
			Winter	0.86 ± 0.17	
	Nam Co	2015	Summer	0.38±0.16	Zhang et al. (Zhang et al.,
India	Delhi	2016	Spring	2.5	Dasari et al. (Dasari et al.,
Korea	Seoul	2012-2013	Winter	1.02	Kim et al. (Kim et al., 2016)
			Summer	0.28	
USA	Los Angeles	2018-2019	Winter	0.7±0.2	Soleimanian et al. (Soleimanian et al., 2020)
			Summer	0.5±0.2	
	Yorkville	2010	Winter	0.41	Hecobian et al. (Hecobian et
	Carolina	2013	Summer	0.29	Mie et al. (Xie et al., 2019)
Switzerland		2013	Winter	0.9	Moschos et al. (Moschos et al., 2018)
			Summer	0.28	
Greece	Ioannina	2019	Summer	0.3 ± 0.1	Paraskevopoulou et al.

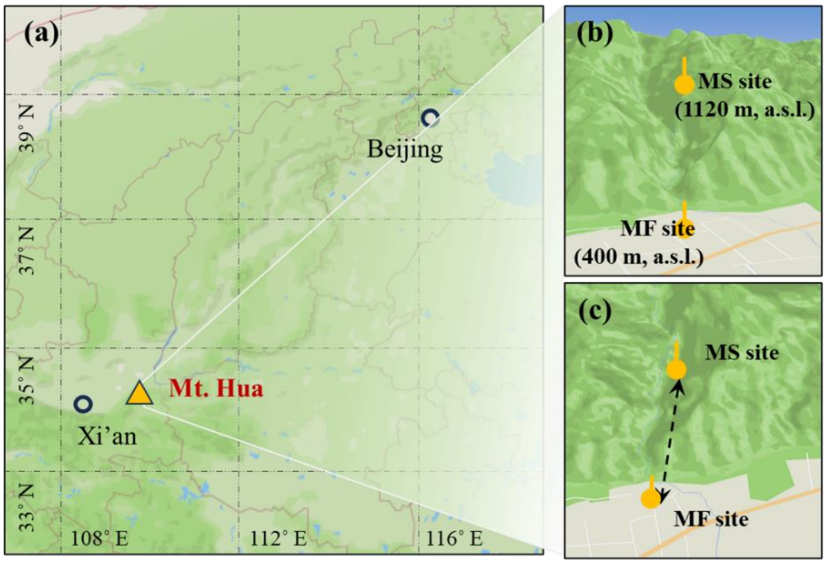

Figure S1. Locations of the sampling sites in China. **(a)** Topographic view, **(b)** vertical view and bird's-eye view **(c)** of Mt. Hua with the sampling sites marked. The maps are the reproductions from ©Mapbox (https://account.mapbox.com/, last access: 16 March 2024)

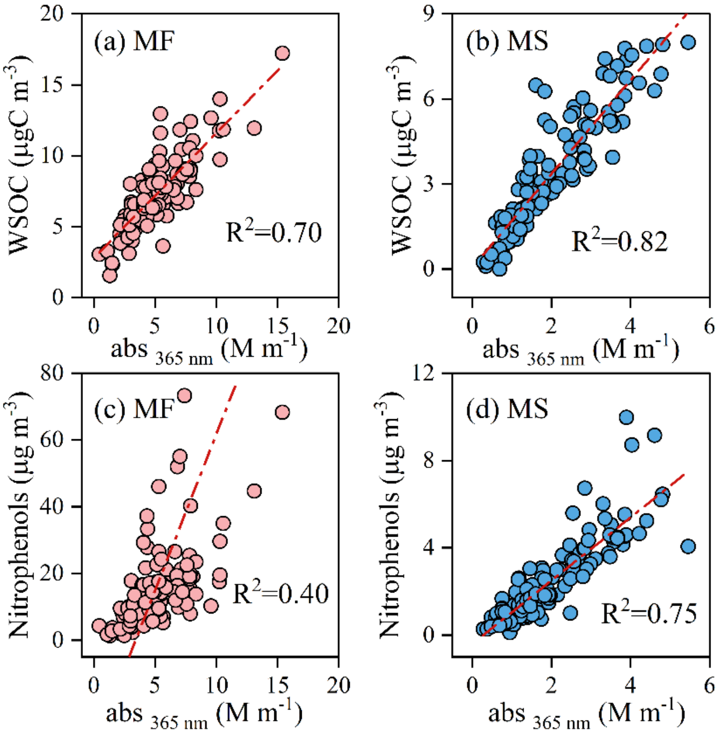

Figure S2. Linear fit regression analysis for Abs $_{\lambda=365\ nm}$ with WSOC and nitrophenols at MF and MS sites

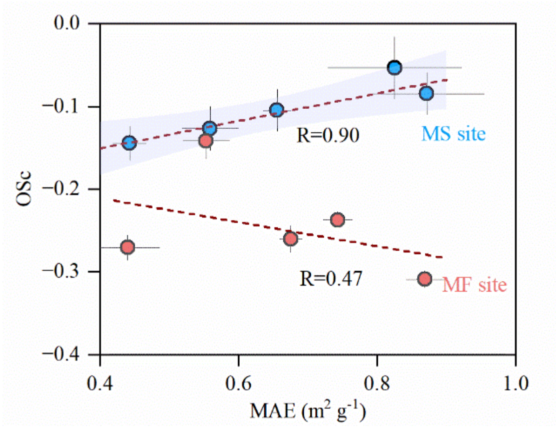

Figure S3. The correlativity between MAE_{365nm} and OSc value at both sampling sites.

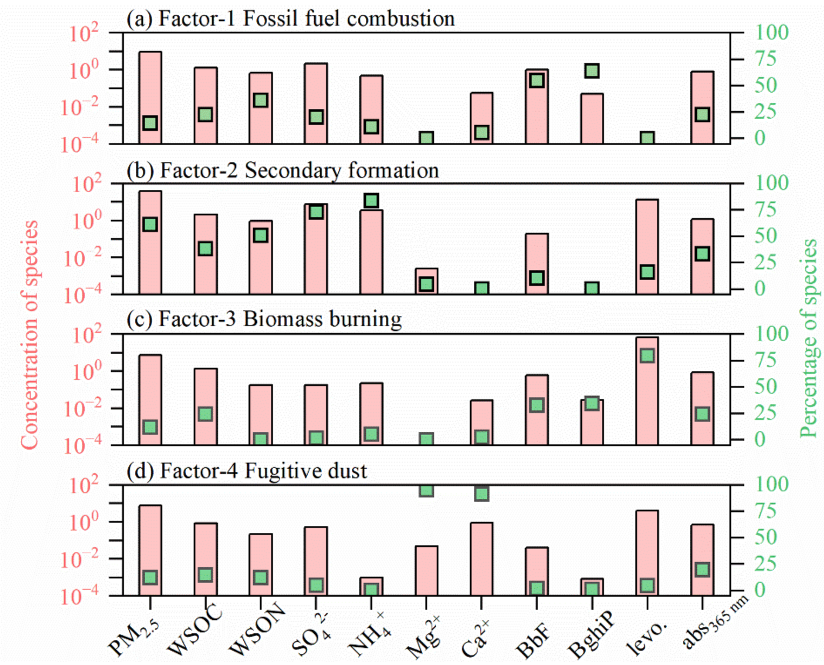

Figure S4. Source apportionment for light absorption of daytime water-soluble BrC ($abs_{365\ nm}$) of all the daytime samples collected during the whole campagin.

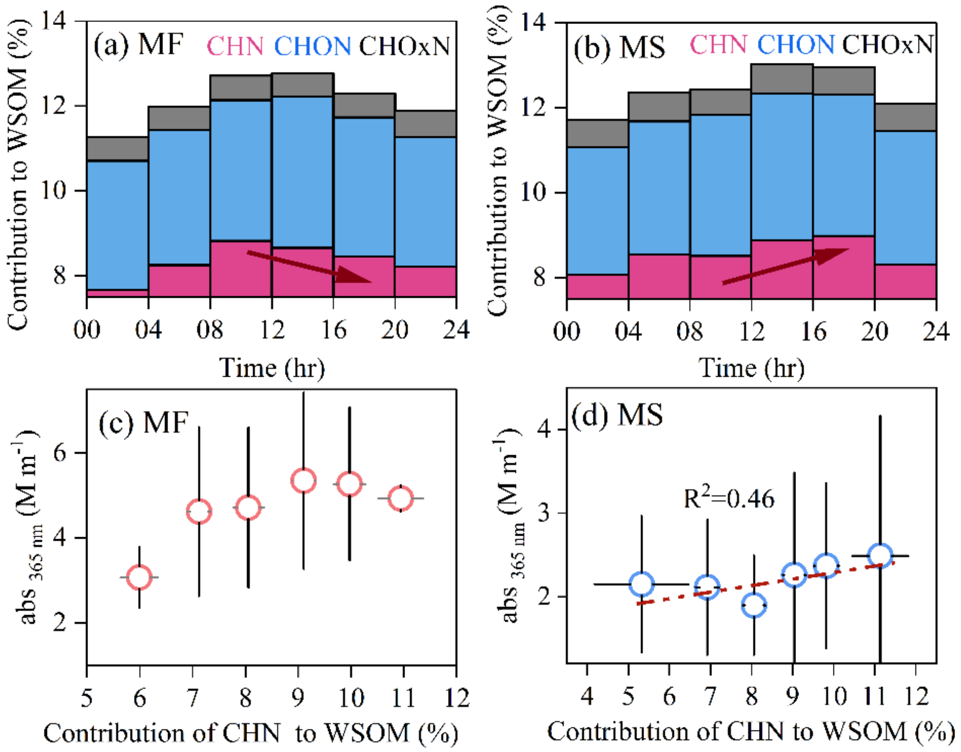

Figure S5. (a) and (b) Diurnal variations in relative contributions of nitrogen-containing organic fragments to WSOM at MF and MS sites, respetively. (c and d) The dependence of light absorption of WSOC (Abs $_{\lambda=365\ nm}$) on the relative contributions of CHN fragments to WSOM at the two sampling sites.

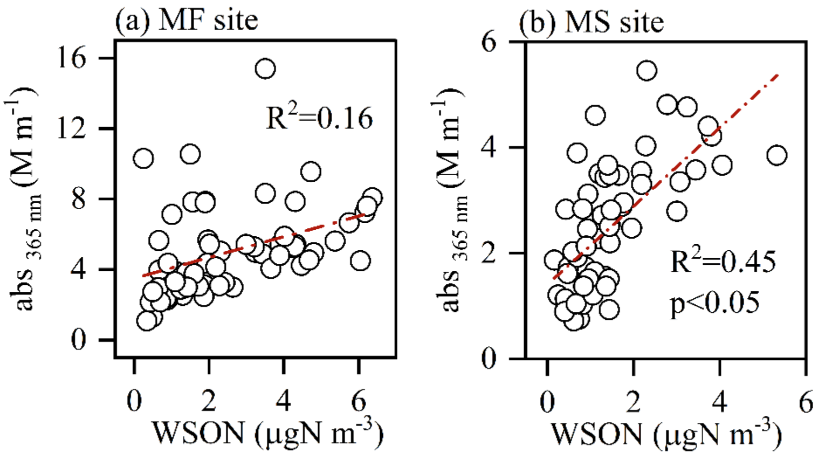

Figure S6 Linear fit regression analysis for Abs $_{\lambda=365\ nm}$ and WSON of the daytime samples at two sites

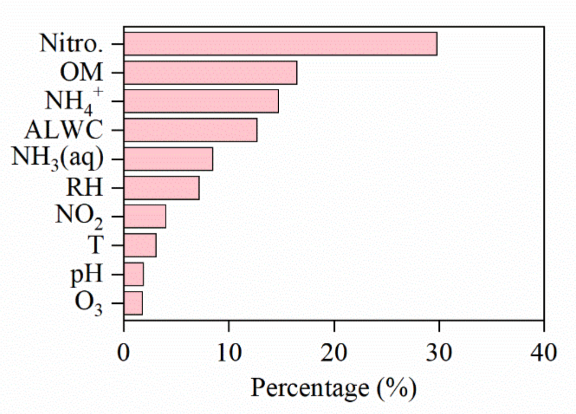

Figure S7 Random forest analysis for daytime WSON of the $PM_{2.5}$ at MF site.

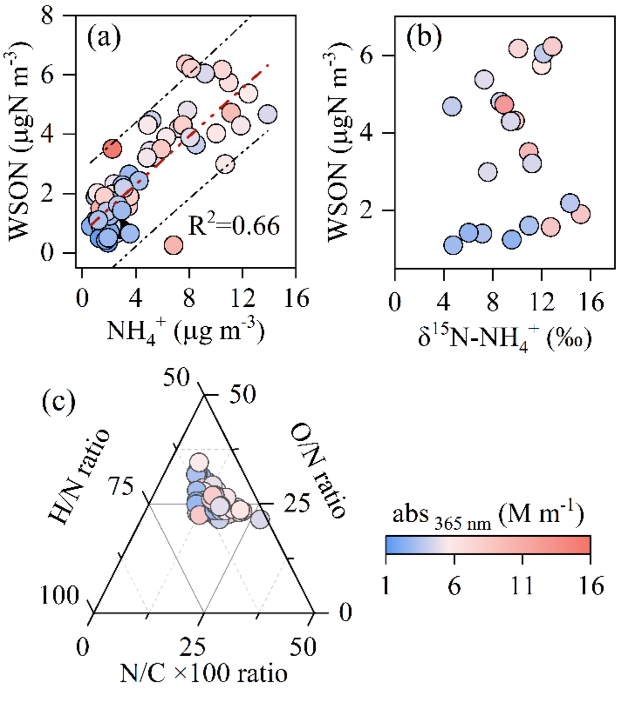

Figure S8 Impacts on WSON formation at MF site. Linear fit regressions for WSON with NH_4^++NH_3(aq) (a) and δ-^{15}N-NH_4^+ (b) at MF site and triangular chart for the elemental ratios of N/C, H/N and O/N of WSOC at MF site (c).

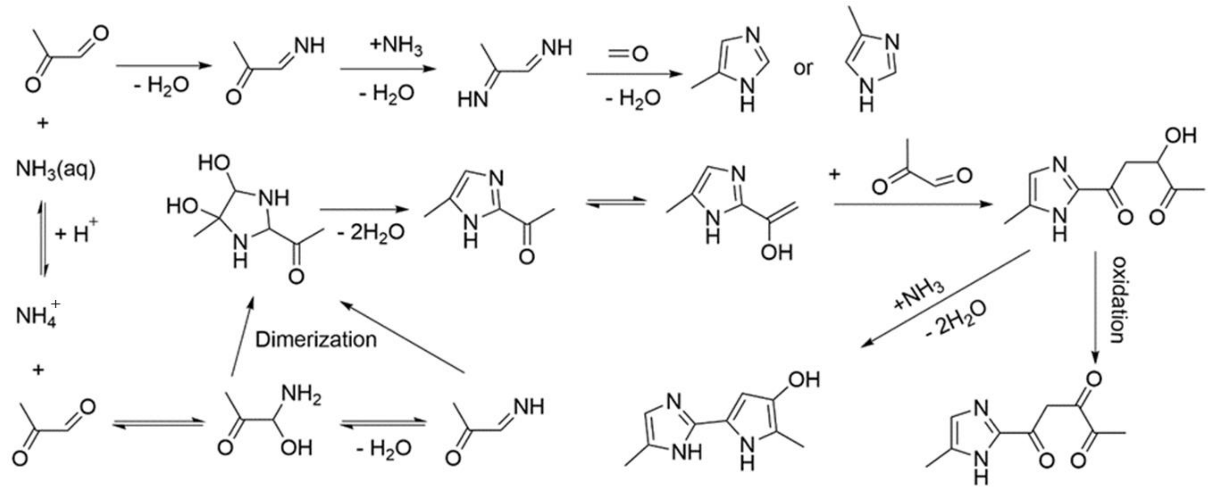

Figure S9 Simple reaction paths for imidazoles or N-heterocycles (Modified from Aiona et al. (2017) and Jang et al. (2013))

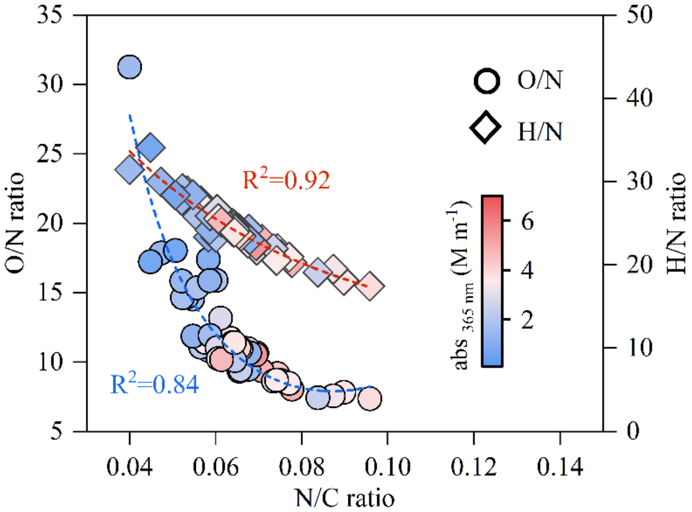

Figure S10 Elemental composition of daytime WSOC at MS site.

References

Aiona, P. K., Lee, H. J., Leslie, R., Lin, P., Laskin, A., Laskin, J., and Nizkorodov, S. A.: Photochemistry of Products of the Aqueous Reaction of Methylglyoxal with Ammonium Sulfate, ACS Earth Space Chem., 1, 522-532, 10.1021/acsearthspacechem.7b00075, 2017.

Cao, J.-J., Zhang, T., Chow, J. C., Watson, J. G., Wu, F., and Li, H.: Characterization of Atmospheric Ammonia over Xi'an, China, Aerosol Air Qual. Res., 9, 277-289, 2009.

Chen, Y., Ge, X., Chen, H., Xie, X., Chen, Y., Wang, J., Ye, Z., Bao, M., Zhang, Y., and Chen, M.: Seasonal light absorption properties of water-soluble brown carbon in atmospheric fine particles in Nanjing, China, Atmos. Environ., 187, 230-240, 10.1016/j.atmosenv.2018.06.002, 2018.

Chen, Y., Xie, X., Shi, Z., Li, Y., Gai, X., Wang, J., Li, H., Wu, Y., Zhao, X., Chen, M., and Ge, X.: Brown carbon in atmospheric fine particles in Yangzhou, China: Light absorption properties and source apportionment, Atmos. Res., 244, 10.1016/j.atmosres.2020.105028, 2020.

Cheng, Y., He, K.-b., Du, Z.-y., Engling, G., Liu, J.-m., Ma, Y.-l., Zheng, M., and Weber, R. J.: The characteristics of brown carbon aerosol during winter in Beijing, Atmos. Environ., 127, 355-364, 10.1016/j.atmosenv.2015.12.035, 2016.

Dasari, S., Andersson, A., Bikkina, S., Holmstrand, H., Budhavant, K., Satheesh, S., Asmi, E., Kesti, J., Backman, J., Salam, A., Bisht, D. S., Tiwari, S., Hameed, Z., and Gustafsson, O.: Photochemical degradation affects the light absorption of water-soluble brown carbon in the South Asian outflow, Science Advances, 5, 10.1126/sciadv.aau8066, 2019.

Deng, J., Ma, H., Wang, X., Zhong, S., Zhang, Z., Zhu, J., Fan, Y., Hu, W., Wu, L., Li, X., Ren, L., Pavuluri, C. M., Pan, X., Sun, Y., Wang, Z., Kawamura, K., and Fu, P.: Measurement report: Optical properties and sources of water-soluble brown carbon in Tianjin, North China insights from organic molecular compositions, Atmos. Chem. Phys., 22, 6449-6470, 10.5194/acp-22-6449-2022, 2022.

Du, Z., He, K., Cheng, Y., Duan, F., Ma, Y., Liu, J., Zhang, X., Zheng, M., and Weber, R.: A yearlong study of water-soluble organic carbon in Beijing II: Light absorption properties, Atmospheric Environment, 89, 235-241, http://dx.doi.org/10.1016/j.atmosenv.2014.02.022, 2014.

He, T., Wu, Y., Wang, D., Cai, J., Song, J., Yu, Z., Zeng, X., and Peng, P. a.: Molecular compositions and optical properties of water-soluble brown carbon during the autumn and winter in Guangzhou, China, Atmos. Environ., 296, 10.1016/j.atmosenv.2022.119573, 2023.

Hecobian, A., Zhang, X., Zheng, M., Frank, N., Edgerton, E. S., and Weber, R. J.: Water-Soluble Organic Aerosol material and the light-absorption characteristics of aqueous extracts measured over the Southeastern United States, Atmos. Chem. Phys., 10, 5965-5977, 10.5194/acp-10-5965-2010, 2010.

Hu, M., Wu, Z., Slanina, J., Lin, P., Liu, S., and Zeng, L.: Acidic gases, ammonia and water-soluble ions in PM2.5 at a coastal site in the Pearl River Delta, China, Atmos. Environ., 42, 6310-6320, 10.1016/j.atmosenv.2008.02.015, 2008.

Jang, H. W., Jiang, Y., Hengel, M., and Shibamoto, T.: Formation of 4(5)-Methylimidazole and Its Precursors, α-Dicarbonyl Compounds, in Maillard Model Systems, J. Agric. Food. Chem., 61, 6865-6872, 10.1021/jf401958w, 2013.

Kim, H., Kim, J. Y., Jin, H. C., Lee, J. Y., and Lee, S. P.: Seasonal variations in the light-absorbing properties of water-soluble and insoluble organic aerosols in Seoul, Korea, Atmos. Environ., 129, 234-242, 10.1016/j.atmosenv.2016.01.042, 2016.

Kuang, Y., Xu, W., Lin, W., Meng, Z., Zhao, H., Ren, S., Zhang, G., Liang, L., and Xu, X.: Explosive morning growth phenomena of NH3 on the North China Plain: Causes and potential impacts on aerosol formation, Environ. Pollut., 257, 10.1016/j.envpol.2019.113621, 2020.

Li, C., Chen, P., Kang, S., Yan, F., Hu, Z., Qu, B., and Sillanpaa, M.: Concentrations and light absorption characteristics of carbonaceous aerosol in PM2.5 and PM10 of Lhasa city, the Tibetan Plateau, Atmos. Environ., 127, 340-346, 10.1016/j.atmosenv.2015.12.059, 2016.

Li, D., Wu, C., Zhang, S., Lei, Y., Lv, S., Du, W., Liu, S., Zhang, F., Liu, X., Liu, L., Meng, J., Wang, Y., Gao, J., and Wang, G.: Significant coal combustion contribution to water-soluble brown carbon during winter in Xingtai, China: Optical properties and sources, J. Environ. Sci., 124, 892-900, 10.1016/j.jes.2022.02.026, 2023a.

Li, J., Zhang, Q., Wang, G., Li, J., Wu, C., Liu, L., Wang, J., Jiang, W., Li, L., Ho, K. F., and Cao, J.: Optical properties and molecular compositions of water-soluble and water-insoluble brown carbon (BrC) aerosols in northwest China, Atmos. Chem. Phys., 20, 4889-4904, 10.5194/acp-20-4889-2020, 2020.

Li, X., Yu, F., Song, Y., Zhang, C., Yan, F., Hu, Z., Lei, Y., Tripathee, L., Zhang, R., Guo, J., Wang, Y., Chen, Q., Liu, L., Cao, J., and Wang, Q.: Water-soluble brown carbon in PM2.5 at two typical sites in Guanzhong Basin: Optical properties, sources, and implications, Atmos. Res., 281, 10.1016/j.atmosres.2022.106499, 2023b.

Liu, J., Mo, Y., Ding, P., Li, J., Shen, C., and Zhang, G.: Dual carbon isotopes (C-14 and C-13) and optical properties of WSOC and HULIS-C during winter in Guangzhou, China, Sci. Total Environ., 633, 1571-1578, 10.1016/j.scitotenv.2018.03.293, 2018.

Lv, S., Wang, F., Wu, C., Chen, Y., Liu, S., Zhang, S., Li, D., Du, W., Zhang, F., Wang, H., Huang, C., Fu, Q., Duan, Y., and Wang, G.: Gas-to-Aerosol Phase Partitioning of Atmospheric Water-Soluble Organic Compounds at a Rural Site in China: An Enhancing Effect of NH3 on SOA Formation, Environ. Sci. Technol., 56, 3915-3924, 10.1021/acs.est.1c06855, 2022.

Meng, Z., Lin, W., Zhang, R., Han, Z., and Jia, X.: Summertime ambient ammonia and its effects on ammonium aerosol in urban Beijing, China, Sci. Total Environ., 579, 1521-1530, 10.1016/j.scitotenv.2016.11.159, 2017.

Meng, Z., Zhang, R., Lin, W., Jia, X., Yu, X., Yu, X., and Wang, G.: Seasonal Variation of Ammonia and Ammonium Aerosol at a Background Station in the Yangtze River Delta Region, China, Aerosol Air Qual. Res., 14, 756-766, 10.4209/aaqr.2013.02.0046, 2014.

Meng, Z., Xu, X., Lin, W., Ge, B., Xie, Y., Song, B., Jia, S., Zhang, R., Peng, W., Wang, Y., Cheng, H., Yang, W., and Zhao, H.: Role of ambient ammonia in particulate ammonium formation at a rural site in the North China Plain, Atmos. Chem. Phys., 18, 167-184, 10.5194/acp-18-167-2018, 2018.

Moschos, V., Kumar, N. K., Daellenbach, K. R., Baltensperger, U., Prevot, A. S. H., and El Haddad, I.: Source Apportionment of Brown Carbon Absorption by Coupling Ultraviolet-Visible Spectroscopy with Aerosol Mass Spectrometry, Environmental Science & Technology Letters, 5, 302-+, 10.1021/acs.estlett.8b00118, 2018.

Pan, Y., Tian, S., Zhao, Y., Zhang, L., Zhu, X., Gao, J., Huang, W., Zhou, Y., Song, Y., Zhang, Q., and Wang, Y.: Identifying Ammonia Hotspots in China Using a National Observation Network, Environ. Sci. Technol., 52, 3926-3934, 10.1021/acs.est.7b05235, 2018.

Paraskevopoulou, D., Kaskaoutis, D. G., Grivas, G., Bikkina, S., Tsagkaraki, M., Vrettou, I. M., Tavernaraki, K., Papoutsidaki, K., Stavroulas, I., Liakakou, E., Bougiatioti, A., Oikonomou, K., Gerasopoulos, E., and Mihalopoulos, N.: Brown carbon absorption and radiative effects under intense residential wood burning conditions in Southeastern Europe: New insights into the abundance and absorptivity of methanol-soluble organic aerosols, Sci. Total Environ., 860, 10.1016/j.scitotenv.2022.160434, 2023.

Soleimanian, E., Mousavi, A., Taghvaee, S., Shafer, M. M., and Sioutas, C.: Impact of secondary and primary particulate matter (PM) sources on the enhanced light absorption by brown carbon (BrC) particles in central Los Angeles, Sci. Total Environ., 705, 10.1016/j.scitotenv.2019.135902, 2020.

Tao, Y., Sun, N., Li, X., Zhao, Z., Ma, S., Huang, H., Ye, Z., and Ge, X.: Chemical and Optical Characteristics and Sources of PM2.5 Humic-Like Substances at Industrial and Suburban Sites in Changzhou, China, Atmosphere, 12, 10.3390/atmos12020276, 2021.

Ting, Y.-C., Ko, Y.-R., Huang, C.-H., Cheng, Y.-H., and Huang, C.-H.: Optical properties and potential sources of water-soluble and methanol-soluble organic aerosols in Taipei, Taiwan, Atmos. Environ., 290, 10.1016/j.atmosenv.2022.119364, 2022.

Wang, D., Shen, Z., Zhang, Q., Lei, Y., Zhang, T., Huang, S., Sun, J., Xu, H., and Cao, J.: Winter brown carbon over six of China's megacities: light absorption, molecularcharacterization, and improved source apportionment revealed by multilayerperceptron neural network, Atmos. Chem. Phys., 22, 14893-14904, 10.5194/acp-22-14893-2022, 2022.

Wang, S., Nan, J., Shi, C., Fu, Q., Gao, S., Wang, D., Cui, H., Saiz-Lopez, A., and Zhou, B.: Atmospheric ammonia and its impacts on regional air quality over the megacity of Shanghai, China, Sci. Rep., 5, 10.1038/srep15842, 2015.

Wen, H., Zhou, Y., Xu, X., Wang, T., Chen, Q., Chen, Q., Li, W., Wang, Z., Huang, Z., Zhou, T., Shi, J., Bi, J., Ji, M., and Wang, X.: Water-soluble brown carbon in atmospheric aerosols along the transport pathway of Asian dust: Optical properties, chemical compositions, and potential sources, Sci. Total Environ., 789, 10.1016/j.scitotenv.2021.147971, 2021.

Wu, C., Cao, C., Li, J., Lv, S., Li, J., Liu, X., Zhang, S., Liu, S., Zhang, F., Meng, J., and Wang, G.: Different physicochemical behaviors of nitrate and ammonium duringtransport: a case study on Mt. Hua, China, Atmos. Chem. Phys., 22, 15621-15635, 10.5194/acp-22-15621-2022, 2022.

Wu, C., Wang, G., Li, J., Li, J., Cao, C., Ge, S., Xie, Y., Chen, J., Liu, S., Du, W., Zhao, Z., and Cao, F.: Non-agricultural sources dominate the atmospheric NH3 in Xi'an, a megacity in the semi-arid region of China, Sci. Total Environ., 722, 137756, 10.1016/j.scitotenv.2020.137756, 2020a.

Wu, C., Lv, S., Wang, F., Liu, X., Li, J., Liu, L., Zhang, S., Du, W., Liu, S., Zhang, F., Li, J., Meng, J., and Wang, G.: Ammonia in urban atmosphere can be substantially reduced by vehicle emission control: A case study in Shanghai, China, J. Environ. Sci., 126, 754-760, 10.1016/j.jes.2022.04.043, 2023.

Wu, C., Wang, G., Li, J., Li, J., Cao, C., Ge, S., Xie, Y., Chen, J., Li, X., Xue, G., Wang, X., Zhao, Z., and Cao, F.: The characteristics of atmospheric brown carbon in Xi'an, inland China: sources, size distributions and optical properties, Atmos. Chem. Phys., 20, 2017-2030, 10.5194/acp-20-2017-2020, 2020b.

Wu, G., Wan, X., Ram, K., Li, P., Liu, B., Yin, Y., Fu, P., Loewen, M., Gao, S., Kang, S., Kawamura, K., Wang, Y., and Cong, Z.: Light absorption, fluorescence properties and sources of brown carbon aerosols in the Southeast Tibetan Plateau, Environ. Pollut., 257, 10.1016/j.envpol.2019.113616, 2020c.

Xie, M., Chen, X., Holder, A. L., Hays, M. D., Lewandowski, M., Offenberg, J. H., Kleindienst, T. E., Jaoui, M., and Hannigan, M. P.: Light absorption of organic carbon and its sources at a southeastern US location in summer, Environ. Pollut., 244, 38-46, 10.1016/j.envpol.2018.09.125, 2019.

Yao, X., Ling, T. Y., Fang, M., and Chan, C. K.: Comparison of thermodynamic predictions for in situ pH in PM2.5, Atmos. Environ., 40, 2835-2844, 10.1016/j.atmosenv.2006.01.006, 2006.

Zhang, Y., Xu, J., Shi, J., Xie, C., Ge, X., Wang, J., Kang, S., and Zhang, Q.: Light absorption by water-soluble organic carbon in atmospheric fine particles in the central Tibetan Plateau, Environmental Science and Pollution Research, 24, 21386-21397, 10.1007/s11356-017-9688-8, 2017.

Zhao, Y., Wu, C., Wang, Y.-q., Chen, Y.-b., Lu, S.-j., Wang, F.-l., Du, W., Liu, S.-j., Ding, Z.-j., and Wang, G.-h.: Pollution Characteristics and Sources of Wintertime Atmospheric Brown Carbon at a Background Site of the Yangtze River Delta Region in China, Huanjing Kexue, 42, 3127-3135, 10.13227/j.hjkx.202012002, 2021.

Zhu, C.-S., Cao, J.-J., Huang, R.-J., Shen, Z.-X., Wang, Q.-Y., and Zhang, N.-N.: Light absorption properties of brown carbon over the southeastern Tibetan Plateau, Sci. Total Environ., 625, 246-251, 10.1016/j.scitotenv.2017.12.183, 2018.

Zou, C., Cao, T., Li, M., Song, J., Jiang, B., Jia, W., Li, J., Ding, X., Yu, Z., Zhang, G., and Peng, P. a.: Measurement report: Changes in light absorption and molecular composition ofwater-soluble humic-like substances during a winter haze bloom-decay processin Guangzhou, China, Atmos. Chem. Phys., 23, 963-979, 10.5194/acp-23-963-2023, 2023.